Polímeros
ISSN 1678-5169 (Online)

https://doi.org/10.1590/0104-1428.20230059

ORIGINAL ARTICLES

Effect of process parameters on the properties of LDPE/sepiolite composites

Priscila da Silva e Souza[1], Ana Maria Furtado de Sousa[2] and Ana Lúcia Nazareth da Silva[1,3]*

[1]Instituto de Macromoleculas Professora Eloisa Mano – IMA, Universidade Federal do Rio de Janeiro – UFRJ, Rio de Janeiro, RJ, Brasil
[2]Instituto de Química – IQ, Universidade do Estado do Rio de Janeiro – UERJ, Rio de Janeiro, RJ, Brasil
[3]Programa de Pós-graduação em Engenharia Ambiental – PEA, Universidade Federal do Rio de Janeiro – UFRJ, Rio de Janeiro, RJ, Brasil
**ananazareth@ima.ufrj.br*

Abstract

This study examines the effect of processing parameters and reactive extrusion on the mechanical, thermal, morphological, and rheological properties of low-density polyethylene (LDPE) and sepiolite composites (LDPE/sepiolite: 95/5 wt/wt) produced by in situ reactive extrusion in a twin-screw extruder. Using a design of experiments, the contribution of the factors reverse mixing elements (RE), maleic anhydride (MA), and dicumyl peroxide (DCP) was determined. The results showed that a better interaction between LDPE and sepiolite phases occurred when reactive extrusion was carried out, leading to a satisfactory balance between mechanical properties and thermal stability behavior. The rheology analysis revealed that a more pronounced solid-like behavior was achieved in the composite prepared by reactive extrusion and in the presence of the filler. The SEM micrographs showed the appearance of a network-like morphology in the composite processed in the presence of additives and sepiolite filler.

Keywords: *low density polyethylene, sepiolite, cross-linking, reactive extrusion, composites.*

How to cite: Souza, P. S., Sousa, A. M. F., & Silva, A. L. N. (2024). Effect of process parameters on the properties of LDPE/sepiolite composites. *Polímeros: Ciência e Tecnologia*, *34*(2), e20240015. https://doi.org/10.1590/0104-1428.20230059

1. Introduction

Low-density polyethylene (LDPE) is extensively used in consumer goods and packaging due to its desired properties, such as toughness, high flexibility, and easy processability[1,2] However, according to Liang[2], some applications are not met solely by neat polymers. In this sense, the addition of nanofillers to the LDPE matrix can enlarge the application window by improving, for instance, its barrier and mechanical properties. Zhang et al.[3] revealed that these improvements are strongly dependent on the interfacial effect between the nanofiller and polymer matrix. The addition of inorganic nanofillers into a polymer matrix to produce a nanocomposite has been found to be an interesting possibility for improving some properties of a polymeric material[4]. In this regard, many types of nanofillers, such as graphene, carbon nanotubes, natural inorganic minerals, and layered double hidroxides, have been used in polymeric nanocomposite developments due to their significant impact on microscale properties, resulting in improved mechanical, thermal, flame retardancy, and barrier properties[5-8].

According to Ballesteros et al.[9], research efforts are still necessary to better understand the interaction between nanoparticles and polymeric matrix to achieve a suitable dispersion and, consequently, desired properties. In particular, lamellar silicate fillers, such as clays (hydrophilic fillers), have low compatibility with nonpolar matrices. One of the most common strategies to reinforce interfacial interactions between clay and nonpolar polymers is to add modified polyolefins bearing polar groups, namely compatibilizers or interfacial agents. For this purpose, maleic anhydride-grafted polyolefins have been widely used as interfacial agents[8,10].

Regarding mineral fillers, such as inorganic clays (*e.g.*, bentonite, halloysite nanotubes, organically modified nanoclays, and sepiolite), these materials have been used as plastic additives to improve mechanical, thermal, and barrier properties[8,11,12]. According to Fashchi and Ostad[13], sepiolite is a fibrous nanofiller with a 2:1 phyllosilicate with a crystalline structure in a needle-like morphology. This nanoparticle has open channels extended along the fiber direction and presents the following theoretical unit cell formula: $Si_{12}Mg_8O_{30}(OH)_4(OH_2)_4.8H_2O$[13,14]. Sepiolite has fiber sizes varying between 0.2 µm to 2 µm in length, 100 nm to 300 nm in width, and 50 nm to 100 nm in thickness[14]. Its porosity and specific area are 0.4 $cm^3.g^{-1}$ and 350 $m^2.g^{-1}$, respectively. As reported by Ajmal et al.[15] this nanofiller has been widely used to improve the thermal and mechanical properties of different polymers, such as polyethylenes, poly(lactic acid) and polyamides.

Composites based on polyolefins and sepiolite have been developed[6,16-18].Within this context, Li et al.[6] studied the effect of the addition of a flame retardant-modified sepiolite

on thermal degradation and fire retardant properties of LDPE matrix. Initially, the sepiolite fiber was acidified and then the flame retardant was added, interacting with the fiber. Next, in an extruder, the modified fiber was blended with the PE.The results of the thermal degradation kinetics analysis and the combustion test showed that the incorporation of the modified fiber with the flame retardant improved the thermal stability and flame retardant property of the final composite.

Singh et al.[12] evaluated the addition of different contents of sepiolite (1 – 10 wt.%) in high-density polyethylene (HDPE) matrix. PE-graf-maleic anhydride (PE-g-MA), varying molar mass and MA content, was used as compatibilizer agent. The results showed that the addition of sepiolite into HDPE matrix up to 10 wt.% increased the complex viscosity values and the viscoelastic behavior as compared to neat HDPE. In the presence of the PE-g-MA, the viscoelastic behavior decreased as compared to uncompatibilized systems at the same filler content. The reduction in the viscoelastic properties was more pronounced in composites with compatibilizer of lower molar mass.

Nuñes et al.[17] studied nanocomposites based on poly(lactic acid) (PLA), low-density polyethylene (LDPE) and sepiolite (SEP). The systems were prepared by corotating twin-screw extruder and using two grafted polymers as compatibilizer agents – a styrene/ethylene-butylene/styrene rubber (SEBS-g-MA) and a grafted polyethylene (PE-g-MA). The addition of sepiolite clay reduced the thermo-oxidative degradation of the neat PLA. The presence of SEP at the PE interface and in the PLA matrix phase reduces the effectiveness of these compatibilizer agents, resulting in lower elongation at break than those of the blends without clay.

García et al.[18] compared the effect of different nanofillers (sepiolite, silica nanoparticles and montmorillonite) as thermal stabilizers in LDPE matrix. The nanocomposites were prepared in a Haake mixer chamber by using a concentrated masterbatch procedure. The results showed a strong stabilization effect for both fibrous (sepiolite) and laminar silicate (montmorillonite), but not for the spherical silica nanoparticles. According to the authors, these results suggested the occurrence of a protective layer against thermos-oxidation on the film surface when sepiolite and montmorillonite were added on LDPE matrix.

Although composites based on polyolefins and sepiolite have been developed, research concerning the effect of reactive extrusion on the compatibility of this nanoclay with LDPE matrix is still limited. Therefore, the goal of this research is to determine whether the amount of grafting additives in reactive extrusion and shear rates during processing influence the LDPE interaction with sepiolite. The factors screw profile and dicumyl peroxide (DCP) and maleic anhydride (MA) contents were investigated using a Factorial 2^3 design. Furthermore, extra experiments were performed to compare the conventional with reactive extrusion. The mechanical, thermal, morphological, and rheological properties of LDPE/Sepiolite composites were assessed, with a particular emphasis on their potential for packaging processing.

2. Materials and Methods

2.1 Materials

Low-density polyethylene (LDPE) commercial-grade 352E is produced by Dow Chemical Company. Sepiolite with a surface area of 300 $m^2.g^{-1}$, an average length of 1–2 μm, and channels with dimensions of 3.6 x 10.6Å was donated by TeaditIndustria e Comércio Ltda. Maleic anhydride (MA), grade STBH9257, and dicumyl peroxide (DCP), grade Retilox 40 SAP, both used as additives for in situ reactive extrusion, were purchased in the local market.

2.2 Design of Experiments (DOE)

The experimental design matrix is shown in Table 1. The experimental code used is A/B/C, where A, B, and C represent, respectively, the actual values of MA, DCP, and RE (the number of reverse elements in zone 4 of the extruder). The amounts of MA (0.5 – 1.0%w) and DCP (0.05 – 1.0%w) were defined based on previous tests. Figure 1 shows the screw extruder used, in which three screw profiles were evaluated in the Zone 4 (compression zone): (i) four KB45 kneading elements (RE:0), (ii) three KB45 kneading elements and one reverse element (RE:1), and (iii) two KB45 kneading elements and two reverse elements (RE:2).Furthermore, neat-LDPE and LDPE with 5% wt/wt sepiolite were processed using a traditional extrusion process so that they could be used as control materials and provide more information for comparison with the reactive extrusion experiments. As shown in Table 2, these additional experiments were coded as LDPE-X and LDPE-SEP-X, where X is the actual value of RE related to levels 0 (level -1) and 2 (level 1), respectively.

Table 1. Design of experiment matrix of Simple Factorial 2^3.

Code A/B/C	Factor code level			Factor actual value		
	MA	DCP	RE	MA	DCP	RE
0.5/0.05/0	-1	-1	-1	0.5	0.05	0
0.5/0.05/2	-1	-1	1	0.5	0.05	2
0.5/0.10/2	-1	1	1	0.5	0.1	0
0.5/0.10/0	-1	1	-1	0.5	0.1	2
0.75/0.075/1 (*)	0	0	0	0.75	0.075	1
1.0/0.05/2	1	-1	1	1.0	0.05	0
1.0/0.05/0	1	-1	-1	1.0	0.05	2
1.0/0.10/0	1	1	-1	1.0	0.1	0
1.0/0.10/2	1	1	1	1.0	0.1	2

(*) center point: replicates three times. All experiments have LDPE: Sepiolite:95:5 ratio (wt.%).

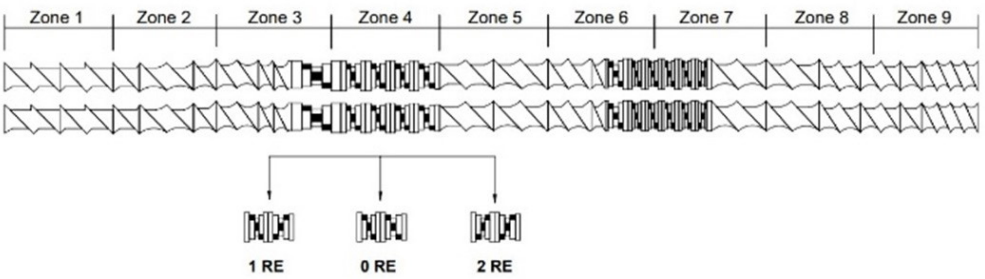

Figure 1. Screw profiles used in the experimental design.

Table 2. Extra experiments.

Code	Factor actual value of RE	LDPE (%wt/wt)	Sepiolite (%wt/wt)
LDPE-0	0	100	-
LDPE-2	2	100	-
SEP-0	0	95	5
SEP-2	2	95	5
gLDPE-2*	2	100	0

* LDPE grafted with 0.5 (wt.%) of MA and 0.10 (wt.%) of DCP.

2.3 Composite preparation

Before extrusion, neat-LDPE and sepiolite were dried for 20 hours in a forced-air oven at 60°C. The neat polymer and all composites were extruded in a Tecktril DCT-20 co-rotating twin screw extruder (L/D: 36 and D:20 mm) at a screw speed of 400 rpm, temperature profile of 90/120/180/185/190/195/200/200/200°C, and feed rate of 18 $kg.h^{-1}$. The raw materials were added simultaneously to the main feeder.

All test specimens were prepared using an Arburg injection-molding machine, model 270S. The temperature profile of the barrel was set at 160/175/185/195/205 °C from feed section to nozzle. The injection pressure and holding pressure were set at 1200 and600 bar, respectively. The cooling time 30 s, and mold temperature of 30°C.

2.4 Characterizations

ATR-FTIR (Attenuated Total Reflection Fourier Transform Infrared) was performed on a Perkin Elmer spectrometer Spectrum One in the 4000 - 400 cm^{-1} range. The purpose of this analysis was to confirm the presence of sepiolite filler in the composites and determine the carbonyl index (*CI*) (Equation 1) in the LDPE matrix[19]:

$$CI = \frac{A_{(1850-1670)}}{A_{(1500-1420)}} \quad (1)$$

Where *CI* is carbonyl index; $A_{(1850–1670)}$ is referred to range of carbonyl group and $A_{(1500–1420)}$ is related to the range of -CH_2 group[19].

The areas under the bands were calculated through the Perkim Elmer software options, using the peak analysis tool.

Dynamic rheological properties of the material were analyzed using an oscillatory rheometer (TA Instruments TRIOS Discovery HR-1 Rheometer, using 25 mm-diameter parallel plates) operating at 200 ºC. The gap between the parallel plates was 1 mm. First, a stress sweep test was conducted to determine the linear viscoelastic region of the material. Next, dynamic frequency sweep tests (oscillatory stress: 100 Pa; frequency range: 0.03 to 600 rad/s) were performed to determine the dynamic properties of the material. The rheological behavior of the samples was evaluated based on their complex viscosity (η*) and storage modulus (G') as a function of frequency (ω).

The cryofractured surface morphology of composites was analyzed by JEOL-1200 scanning electron microscope (SEM). The elements (Mg and Si) from sepiolite were mapped by using the EDS (energy-dispersive X-ray spectroscopy) accessory, Thermo Scientific model 5225 Verona Road, coupled to the SEM microscope.

Tensile tests were performed using a universal testing machine (EMIC, model DL3000) following ASTM D638 (Type I). The crosshead speed was 50 $mm.min^{-1}$. The results were also averaged over five replicates of each composition.

Thermal stability was evaluated by thermogravimetric analysis (TGA) using a Q500 analyzer (TA Instruments). About 15 mg of sample was analyzed at a heating rate of 10 °C.min^{-1} from 25 to 900 °C under N_2 atmosphere. The temperatures at weight loss onset (T_{ONSET}) and maximum degradation rate (T_{MAX}) were determined.

3. Results and Discussions

3.1 Fourier-transform infrared spectroscopy (ATR-FTIR)

Sepiolite is a 2:1 microfibrous tri-octahedral silicate mineral with the formula $Si_{12}Mg_8O_{30}(OH)_4(OH_2)_4.nH_2O$. It is composed of polysomes and channels that extend along the direction of the fiber. The polysomes are composed of an octahedral sheet containing Mg and linked by inversion of tetrahedrons through Si-O-Si bonds, called siloxane bridges, surrounded by two silica tetrahedral sheets, which form continuous tetrahedral sheets with the apices on adjacent polysomes pointing in opposite directions. The absorption bands at 976, 1010 and 1210 cm^{-1} in the ATR-FTIR spectra (Figure 2) are ascribed to the siloxane bridges (Si-O-Si) of sepiolite[19].

Further, the bands around 3640 and 1620 cm^{-1} are attributed to the stretching and bending vibrations of water molecules, respectively. In the range of 900–600 cm^{-1},

the absorption bands can be attributed to the vibrations of hydroxyl groups associated with octahedral $Mg^{2+}$and water molecules of the bound type. The bands with shoulders at 535 and 500 $cm^{-1}$are related to the deformation vibrations in tetrahedral sheets[18]. According to Zhang et al.[3], there are three types of water in sepiolite: zeolitic water within the channels varying with relative humidity, coordinated water molecules binding to the terminal Mg atoms, and structural water referring to the OH^- groups of the octahedral sheet as phyllosilicate.

The superposition of the LDPE and g-LDPE spectra and the integrating areas are shown in Figure 3. Table 3 shows the *CI* calculated using Equation 1.

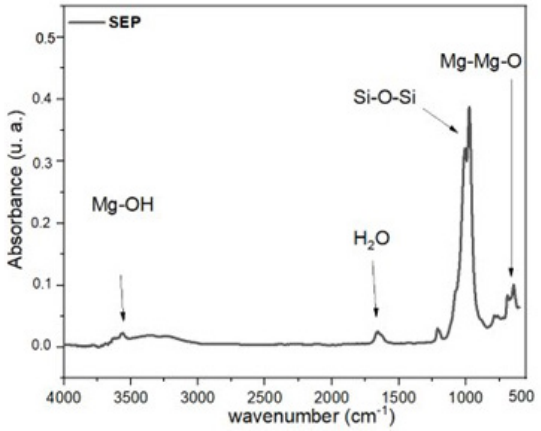

Figure 2. ATR-FTIR spectra of sepiolite (SEP).

According to Almond et al.[19], the *CI* index was determined from the ratio between the integrated band absorbance of the carbonyl (C=O) peak (1850 –1670 cm^{-1}) and of methylene (CH_2) scissoring peak (1500 – 1420 cm^{-1}). As can be seen in Figure 3b, the peak which appears in the range 1850-1670 $cm^{-1}$is very small, almost non-existent. In Figure 3c it is already possible to identify characteristic carbonyl bands. On the other hand, in the FTIR of the gLDPE-2 sample, the absorbance intensity at wavenumber of 1466 cm^{-1} (related to CH_2 band) is smaller than that of LDPE-2, which leads to a higher *CI* value for the gLDPE-2 sample, signaling the occurrence of a grafting process.

Figure 3b exhibits a peak at around 1640 cm^{-1}, associated with amines incorporated into polyethylene resins as UV stabilizers as HAS (Hindered Amine Stabilizers)[20]. This peak is not present in the material after reactive extrusion. A possible reason for this finding is that the grafting additives underwent a reaction with the amine groups during the reactive extrusion, thereby shielding the amine groups.

3.2 Oscillatory rheology and SEM microscopy

The frequency dependency of the storage modulus (G') and loss modulus (G") of the materials determined from frequency (ω) sweep analysis is shown in Figure 4, which

Table 3. Carbonyl index of LDPE and g-LDPE.

Sample Code	Integrated area of		Carbonyl index (*CI*)
	1850 – 1670 cm^{-1}	1500 – 1420 cm^{-1}	
LDPE	0.06	2.91	0.026
g-LDPE	0.19	2.30	0.083

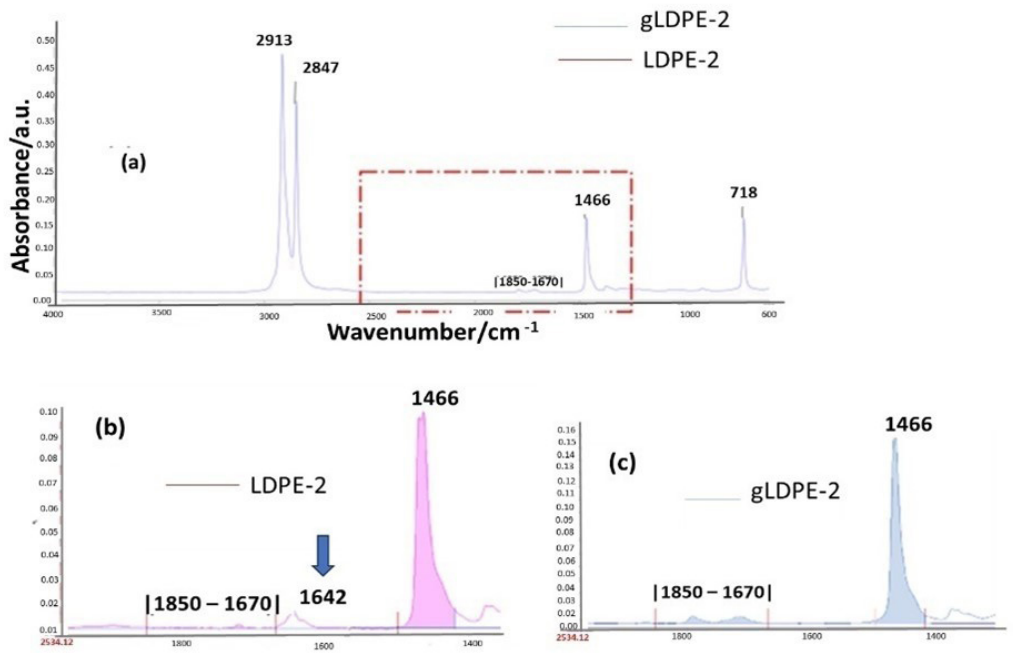

Figure 3. ATR-FTIR spectra of (a) LDPE-2 and gLDPE-2; (b) LDPE-2 (*zoom* at 2500– 1300 cm^{-1}) and (c) gLDPE-2 (*zoom* at 2500 – 1300 cm^{-1}).

also shows the micrographs from SEMand the EDS images (scoring the Si element).

Table 4 shows the values of the crossover point, at which G' = G", determined from G' and G" *versus* the frequency curves. The decrease in both G'=G" and ω_c values of SEP-2 relative to LDPE-2 shows that the addition of sepiolite filler led to an increase in the elastic behavior, signaling the reinforcing effect of the clay in the LDPE matrix.

Further, comparing LDPE-2 to LDPE processed by reactive extrusion (gLDPE-2), it can be seen that gLDPE-2 presented higher elastic behavior in the whole frequency range analyzed, confirming the occurrence of the grafting reaction during processing. When sepiolite was added in the presence of MA/DCP additives, a composition with a more pronounced elastic behavior was produced, showing the effect of the grafting reaction in the interaction of LDPE and filler phases. These results corroborate the findings shown in the SEM micrographs and EDS images (Figure 4). As can be seen, LDPE-SEP-2 and 0.5/0.10/2 composite have different morphologies. The 0.5/0.10/2 composite shows a different morphology, conforming the occurrence of the grafting reaction in the LDPE matrix. In addition, it is also possible to observed that the dispersion of the sepiolite (indicated by Si element, marked with red points) was more efficient in the composition processed by reaction extrusion (see Figure S1 in Supplementary Material).The improved dispersion was confirmed by EDS images, which show that sepiolite dispersion increases in samples from reactive extrusion. It is important to highlight the role of reverse elements in the dispersion/distribution mechanism of sepiolite in the LDPE matrix. The greater residence time achieved due to the presence of these mixing elements allowed greater efficiency in the grafting process and, consequently, leading to better dispersion of the filler in the LDPE matrix.

Table 4. Dynamic modulus and frequency values at the G'/G" crossover point for neat LDPE and LDPE compositions.

Sample code	Modulus at crossover point G' = G"	Crossover point ω_c (rad s^{-1})
LDPE-2	15,500	15.40
SEP-2	8,800	0.10
gLDPE-2	-	-
0.5/0.10/2	-	-

According to Jian et al.[21], the dependence of G' on frequency can indicate the dynamics of the polymer chain structure. For instance, a homopolymer with a narrow molecular weight will present the terminal behavior of the G'α ω^2 curve. Based on the present experimental data, neat LDPE (processed without the presence of MA/DCP additives) deviated from standard terminal behavior, showing G' α $\omega^{0.60}$ (R^2=0.98). When sepiolite was added to

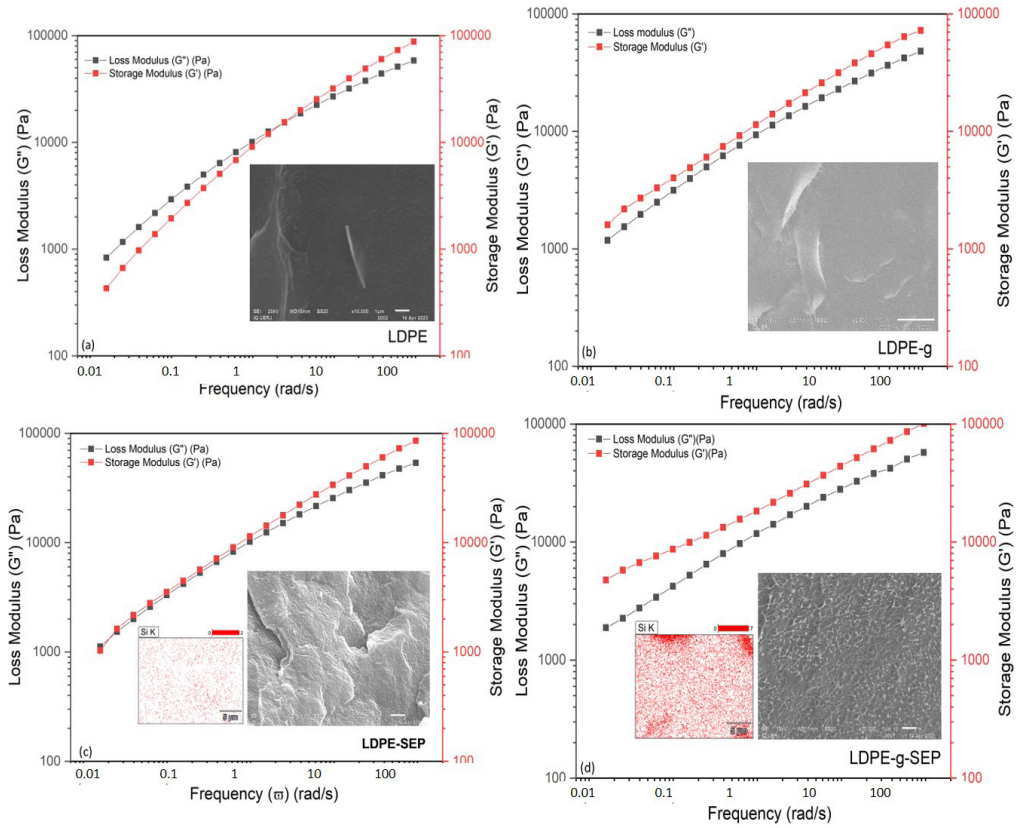

Figure 4. Storage modulus (G') and Loss modulus (G") as a function of frequency a) LDPE-2, b) gLDPE-2, c) SEP-2 and d) 0.5/0.10/2 composite.SEM micrographs and EDS (Si element) images.

the LDPE matrix, the relationship between G' and ω was G' α $\omega^{0.49}$ (R^2=0.99), indicating an increase in the elastic behavior of the LDPE-SEP composition. When LDPE was processed by reactive extrusion (gLDPE-2), the relationship between G' and ω was G' α $\omega^{0.44}$ (R^2=0.99), showing a more pronounced elastic behavior. The 0.5/0.10/2 composite showed the relationship G' α $\omega^{0.35}$ (R^2=0.99), indicating that this sample presented a more pronounced improvement in solid-like behavior compared to others, probably due to the higher interaction between the LDPE matrix and sepiolite phases achieved[22,23].

Figure 5 shows the complex shear viscosities (η*) as a function of the frequency forLDPE-2, SEP-2,gLDPE-2, and 0.5/0.10/2 samples.

LDPE exhibits the lowest viscosities at low frequencies. When sepiolite filler is added to the LDPE matrix (SEP-2), higher viscosity values are achievedat low frequencies comparedto LDPE, signaling the reinforcing effect of the filler in the matrix. The reactive extrusion processing of neat LDPE (gLDPE-2) led to higher viscosity values compared to LDPE, demonstrating the occurrence of the grafting reaction. The reactive extrusion of LDPE with sepiolite led to a pronounced increase in the viscosity values, showing again the effect of the grafting process in the interaction between LDPE matrix and sepiolite filler. In addition, although higher viscosity values are achieved at lower frequencies in 0.5/0.10/2 composition, a shear thinning behavior is observed as frequency was raised. This signals that the composition has an elastic behavior at low frequencies, but as shear rate increases, a decrease in the elastic behavior starts to appear, increasing the flow property of the material. This behavior indicates the potential of use of 0.5/0.10/2 composition in packaging processing. Almeida et al. [24] revealed that high polymer melt strength ensures good bubble stability required by the film blowing process. On the other hand, the material must be sufficiently deformable so that it is able to expand into the formation of the bubble. Thus, the rheological behavior of 0.5/0.10/2 composition indicates its potential use in packaging processing.

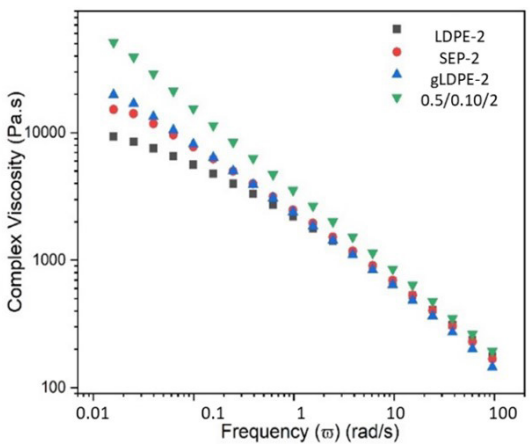

Figure 5. Complex viscosity (η*) as a function of frequency.

3.3 Mechanical and thermal properties

Table 5 shows the elastic modulus, yield stress, and strain at break for the LDPE composites and the control experiments.

Figure 6 shows the graphics produced by the analysis of DOE for elastic modulus. According to the Pareto chart

Table 5. Mechanical properties of neat LDPE and LDPE compositions.

Code MA/ DCP/RE	Elastic modulus (MPa)	Yield stress (MPa)	Strain at break (%)
0.5/0.05/0	167 ± 5	9.2 ± 0.2	64 ± 1
0.5/0.05/2	168 ± 5	9.3 ± 0.2	64 ± 1
0.5/0.10/2	173 ± 5	9.6 ± 0.2	65 ± 1
0.5/0.10/0	174 ± 5	9.1 ± 0.2	65 ± 1
0.75/0.075/1	164 ± 5	8.9 ± 0.2	65 ± 1
1.0/0.05/2	166 ± 5	8.9 ± 0.2	66 ± 1
1.0/0.05/0	160 ± 5	8.8 ± 0.2	65 ± 1
1.0/0.10/0	172 ± 5	9.0 ± 0.2	63 ± 1
1.0/0.10/2	163 ± 5	9.2 ± 0.2	64 ± 1
Extra Experiments used as control			
LDPE-0	121 ± 4	8.5 ± 0.2	75 ± 3
LDPE-2	124 ± 4	8.9 ± 0.2	78 ± 3
SEP-0	132 ± 5	9.1 ± 0.3	62 ± 2
SEP-2	137 ± 5	9.3 ± 0.3	62 ± 2

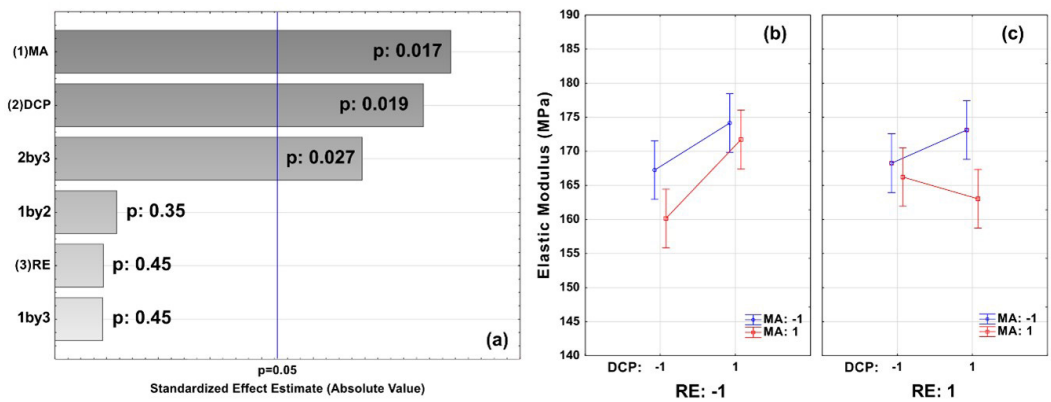

Figure 6. Plots of Simple Factorial 2^3 design of Elastic modulus (a) Pareto Chart and (b-c) Means and Confidence intervals.

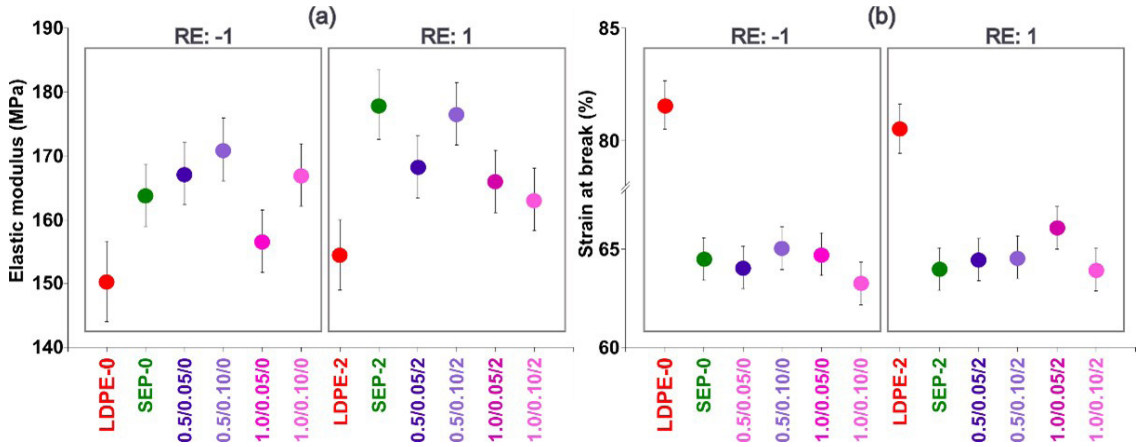

Figure 7. The means and 95% confidence intervals for (a) the elastic modulus and (b) the strain at break of the reactive extrusion experiments and the control experiments.

(Figure 6a), MA affects the elastic modulus first, followed by DCP and the interaction between DCP with RE (2by3). At a RE level of -1 (Figure 6b), there is a slight boost in elastic modulus when the DCP content is increased from -1 to 1. However, a opposing finding is observed when the RE level is +1 (Figure 6c), where the increase in DCP only leads to a rise in the elastic modulus at the MA level of 0.5%wt (level:-1).

Different from what is observed for elastic modulus, the yield stress and strain at break of the LDPE/sepiolite composite produced via reactive extrusion are not impacted by any of the factor tested (MA, DCP, and RE) or their interactions since all p-values are higher than 0.05.

Figure 7 shows the comparison the elastic modulus and strain at break for all composites, with the intervals based on Fisher's least significant difference (LSD) procedure. If two composites have the same property, their intervals will overlap 95% of the time.

The elastic modulus of neat-LDPE (LDPE-0 and LDPE-2) are unaffected by ER, as shown in Figure 7. Adding sepiolite to LDPE via conventional extrusion (SEP-0 and SEP-2) increases the elastic modulus compared to neat-LDPE, regardless the number of reverse elements, signalling the reinforcing effect of sepiolite in the LDPE matrix. When comparing composites processed through reactive extrusion with those processed through conventional extrusion, it is evident that the increase in the elastic modulus is not substantial. Regardless of the extrusion process, all composites exhibited a reduction in strain at break compared to LDPE, indicating a decrease in ductility. Thus, it can be inferred that the changes in the these mechanical properties of LDPE composites are a result of the reinforcement provided by sepiolite, while the modification of LDPE with MA/DCP does not have a substantial impact on these changes.

DOE analysis revealed that process parameters RE (p-value: 0.6), MA content (p-value: 0.4), and DCP content (p-value: 0.4) had no influence on T_{MAX}, i.e., the range of analyzed process parameters had no significant impact on the thermal stability of the composites produced (TGA curvesare presentedin Figure S3 in Supplementary Material). Figure 8 shows a bar chart

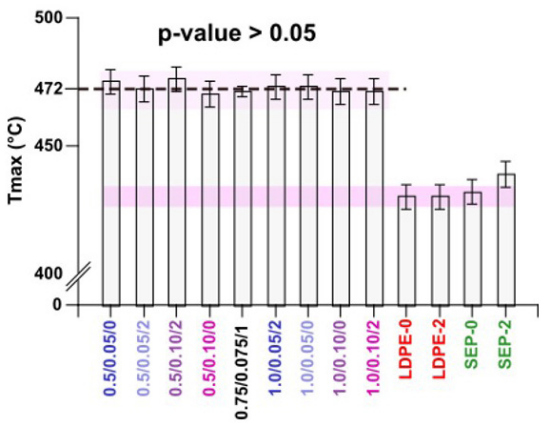

Figure 8. Temperature at maximum degradation rate (T_{MAX}) - Bar Chart Plot, where SEP-0 is LDPE-SEP without reverse elements and SEP-2 is LDPE-SEP processed with 2 (two) reverse elements.

of the temperature at maximum degradation rate (T_{MAX}) of the LDPE/sepiolite composites and the control experiments. The T_{MAX} values of SEP-0 and SEP-2 composites (Figure 8) are observed to be at around 472 °C on average (the standard error of each predicted value is 2 °C), which is nearly 30 °C higher than the T_{MAX} of neat-LDPE (LDPE-0 and LDPE-2). In addition, the grafting composites also present higher T_{MAX} values comparing to composites without AM/DCP (SEP-0 and SEP-2). This behavior can be attribute to the grafting reaction produced during reactive extrusion. It is important to highlight that the 0.5/0.10/2 composite tends to present a slightly higher thermal stability in relation to the other composites processed in the presence of the additives.

From DOE analysis, it was defined that the better experimental conditions that lead to a composition with an optimum balance between mechanical and thermal properties are a higher amount of DCP and lower MA content, using a higher number of RE in the screw profile.

4. Conclusions

This study revealed that the contents of grafting additives and screw profile affected the interaction between the LDPE and sepiolite phases. According to the Fatorial 2^3 design, the optimum balance between mechanical and thermal stability behavior was achieved for the 0.5/0.10/2 composition.

The comparison of 0.5/0.10/2 composition with extra experiments by ATR-FTIR analysis showed that the occurrence of the grafting reaction was efficient, and that the presence of sepiolite filler did not inhibit the grafting mechanism in the LDPE matrix. The micrographs obtained through scanning electron microscopy (SEM) and EDS imagens showed different morphologies between the compositions prepared with and without grafting additives.

The EDS images showed a better dispersion of the sepiolite in the composition prepared by reactive extrusion. Beyond this, the oscillatory rheology test showed a more pronounced elastic behaviour in 0.5/0.10/2 composition, signaling the effect of the grafting reaction in the interaction between LDPE and filler phases. The 0.5/0.10/2 composite presented suitable rheological characteristics to be used in blow process, signaling its potential use in packaging processing.

5. Author's Contribution

- **Conceptualization** – Priscila da Silva e Souza; Ana Maria Furtado de Sousa; Ana Lúcia Nazareth da Silva.
- **Data curation** – Priscila da Silva e Souza.
- **Formal analysis** – Priscila da Silva e Souza;
- **Funding acquisition** – Ana Maria Furtado de Sousa; Ana Lúcia Nazareth da Silva.
- **Investigation** – Priscila da Silva e Souza.
- **Methodology** – Ana Maria Furtado de Sousa; Ana Lúcia Nazareth da Silva.
- **Project administration** – Priscila da Silva e Souza; Ana Maria Furtado de Sousa; Ana Lúcia Nazareth da Silva.
- **Resources** – Priscila da Silva e Souza; Ana Maria Furtado de Sousa; Ana Lúcia Nazareth da Silva.
- **Software** – NA.
- **Supervision** – Ana Maria Furtado de Sousa; Ana Lúcia Nazareth da Silva.
- **Validation** – Priscila da Silva e Souza; Ana Maria Furtado de Sousa; Ana Lúcia Nazareth da Silva.
- **Visualization** – Priscila da Silva e Souza.
- **Writing – original draft** – Priscila da Silva e Souza.
- **Writing – review & editing** – Ana Maria Furtado de Sousa; Ana Lúcia Nazareth da Silva.

6. Acknowledgements

This work was supported by Conselho Nacional de Desenvolvimento Científico e Tecnológico – CNPQ [09461/2021-9 and 307889/2022] Fundação de Amparo à Pesquisa do Estado do Rio de Janeiro – FAPERJ [E-26/010.002212/2019 and E-6/010.001927/2019] and Coordenação de Aperfeiçoamento de Pessoal de Nível Superior - CAPES [Financing code 001]. The authors acknowledge Nitriflex and Lapinus for donating the raw-materials. The Conselho Nacional de Desenvolvimento Científico e Tecnológico (CNPQ) and Fundação de Amparo à Pesquisa do Estado do Rio de Janeiro (FAPERJ) for research supporting.

7. References

1. Dintcheva, N. T., Alessi, S., Arrigo, R., Przybytniak, G., & Spadaro, G. (2012). Influence of the e-beam irradiation and photo-oxidation aging on the structure and properties of LDPE-OMMT nanocomposite films. *Radiation Physics and Chemistry*, *81*(4), 432-436. http://doi.org/10.1016/j.radphyschem.2011.12.018.
2. Liang, J. (2019). Melt strength and drawability of HDPE, LDPE and HDPE/LDPE blends. *Polymer Testing*, *73*, 433-438. http://doi.org/10.1016/j.polymertesting.2018.12.007.
3. Zhang, Q., Li, S., Hu, X., Wang, P., Zeng, J., Wang, X., & Wang, Y. (2017). Structure, morphology, and properties of LDPE/sepiolite nanofiber nanocomposite. *Polymers for Advanced Technologies*, *28*(8), 958-964. http://doi.org/10.1002/pat.3703.
4. Anh, T. T., Fréchette, M., David, É., Veillette, R., & Moraille, P. (2018). Effect of POSS-grafted titanium dioxide on the electrical and thermal properties of LDPE/TiO2 polymer nanocomposite. *Journal of Applied Polymer Science*, *135*(14), 46095. http://doi.org/10.1002/app.46095.
5. Tabatabaei-Yazdi, Z., & Mehdipour-Ataei, S. (2015). Poly(ether-imide) and related sepiolite nanocomposites: investigation of physical, thermal, and mechanical properties. *Polymers for Advanced Technologies*, *26*(4), 308-314. http://doi.org/10.1002/pat.3444.
6. Li, W., Li, S., Cheng, Z., Hu, X., Yang, W., & Yao, Y. (2019). The effect of flame retardant-modified sepiolite nanofibers on thermal degradation and fire retardancy of low-density polyethylene. *Journal of Thermal Analysis and Calorimetry*, *138*(2), 1011-1019. http://doi.org/10.1007/s10973-019-08162-3.
7. Delva, L., Ragaert, K., Degrieck, J., & Cardon, L. (2014). The effect of multiple extrusions on the properties of montmorillonite filled polypropylene. *Polymers*, *6*(12), 2912-2927. http://doi.org/10.3390/polym6122912.
8. Sarifuddin, N., Ismail, H., & Ahmad, Z. (2014). Influence of halloysite nanotubes hybridized with kenaf core fibers on the physical and mechanical properties of low density polyethylene/thermoplastic sago starch blends. *Polymer-Plastics Technology and Engineering*, *53*(2), 107-115. http://doi.org/10.1080/03602559.2013.820758.
9. Ballesteros, A., Laguna-Gutierrez, E., Puertas, M. L., Esteban-Cubillo, A., Santaren, J., & Rodriguez-Perez, M. A. (2021). Polystyrene/sepiolites nanocomposite foams. relationship between composition, particle dispersion, extensional rheology, and cellular structure. *Materials Today. Communications*, *29*, 102850. http://doi.org/10.1016/j.mtcomm.2021.102850.
10. Julinawati, W., Wirjosentono, B., Eddiyanto, E., Gea, S., & Ramli, I. (2020). Morphology and thermal properties of polypropylene-montmorillonite nanocomposite using modified bentonite of Bener Meriah Aceh. *Journal of Natural*, *20*(3), 56-60. http://doi.org/10.24815/jn.v20i3.15073.
11. Rathnam, V., Kichu, A., Dutta, N., Maji, T. K., & Devi, N. (2022). Influence of organically modified nanoclay and TiO2 nanopowder on the properties of Azadirachta indica wood flour-reinforced high-density polyethylene, low-density polyethylene, polypropylene, and polyvinyl chloride nanocomposite. *Journal of Thermoplastic Composite Materials*, *35*(10), 1468-1487. http://doi.org/10.1177/0892705720935968.

12. Singh, V. P., Vimal, K. K., Sharma, S., Kapur, G. S., & Choudhary, V. (2017). Polyethylene/sepiolite clay nanocomposites: effect of clay content, compatibilizer polarity, and molar mass on viscoelastic and dynamic mechanical properties. *Journal of Applied Polymer Science*, *134*(33), 45197. http://doi.org/10.1002/app.45197.
13. Farshchi, N., & Ostad, Y. K. (2020). Sepiolite as a nanofiller to improve mechanical and thermal behavior of recycled high-density polyethylene. *Progress in Rubber, Plastics and Recycling Technology*, *36*(3), 185-195. http://doi.org/10.1177/1477760620918596.
14. Chen, H., Zheng, M., Sun, H., & Jia, Q. (2007). Characterization and properties of sepiolite/polyurethane nanocomposites. *Materials Science and Engineering A*, *445–446*, 725-730. http://doi.org/10.1016/j.msea.2006.10.008.
15. Ajmal, A. W., Masood, F., & Yasin, T. (2018). Influence of sepiolite on thermal, mechanical and biodegradation properties of poly-3-hydroxybutyrate-co-3-hydroxyvalerate nanocomposites. *Applied Clay Science*, *156*, 11-19. http://doi.org/10.1016/j.clay.2018.01.010.
16. Rehman, S. U., Javaid, S., Shahid, M., Gul, I. H., Rashid, B., Szczepanski, C. R., Naveed, M., & Curley, S. J. (2022). Polystyrene-sepiolite clay nanocomposites with enhanced mechanical and thermal properties. *Polymers*, *14*(17), 3576. http://doi.org/10.3390/polym14173576. PMid:36080650.
17. Nuñes, F. C., Ribeiro, K. C., Martini, F. A., Barrioni, B. R., Santos, J. P. F., & Carvalho, B. M. (2021). PBAT/PLA/cellulose nanocrystals biocomposites compatibilized with polyethylene grafted maleic anhydride (PE-g-MA). *Journal of Applied Polymer Science*, *138*(45), 51342. http://doi.org/10.1002/app.51342.
18. García, N., Hoyos, M., Guzmán, J., & Tiemblo, P. (2009). Comparing the effect of nanofillers as thermal stabilizers in low density polyethylene. *Polymer Degradation & Stability*, *94*(1), 39-48. http://doi.org/10.1016/j.polymdegradstab.2008.10.011.
19. Almond, J., Sugumaar, P., Wenzel, M. N., Hill, G., & Wallis, C. (2020). Determination of the carbonyl index of polyethylene and polypropylene using specified area under band methodology with ATR-FTIR spectroscopy. *E-Polymers*, *20*(1), 369-381. http://doi.org/10.1515/epoly-2020-0041.
20. Gulmine, J. V., Janissek, P. R., Heise, H. M., & Akcelrud, L. (2002). Polyethylene characterization by FTIR. *Polymer Testing*, *21*(5), 557-563. http://doi.org/10.1016/S0142-9418(01)00124-6.
21. Jiang, L., Zhang, J., & Wolcott, M. P. (2007). Comparison of polylactide/nano-sized calcium carbonate and polylactide/montmorillonite composites: reinforcing effects and toughening mechanisms. *Polymer*, *48*(26), 7632-7644. http://doi.org/10.1016/j.polymer.2007.11.001.
22. Ogorodova, L. P., Kiseleva, I. A., Vigasina, M. F., Kabalov, Y. K., Grishchenko, R. O., & Mel'Chakova, L. V. (2014). Natural sepiolite: enthalpies of dehydration, dehydroxylation, and formation derived from thermochemical studies. *The American Mineralogist*, *99*(11–12), 2369-2373. http://doi.org/10.2138/am-2014-4804.
23. Elbourne, A., Truong, V. K., Cheeseman, S., Rajapaksha, P., Gangadoo, S., Chapman, J., & Crawford, R. J. (2019). *The use of nanomaterials for the mitigation of pathogenic biofilm formation.* In V. Gurtler, A. S. Ball, & S. Soni (Eds.), *Methods in Microbiology: Nanotechnology* (pp. 61-92). UK: Academic Press. http://doi.org/10.1016/bs.mim.2019.04.002
24. Almeida, K. M., Sousa, A. M. F., Souza, F. G., Jr., Bertolino, L. C., Rocha, M. C. G., Peres, A. C. C., Ossig, A., & Silva, A. L. N. (2017). Melt rheology and morphology of binary and ternary PS/HIPS blends for blown film extrusion applications. *Polymer Testing*, *64*, 277-286. http://doi.org/10.1016/j.polymertesting.2017.10.016.

Received: Aug. 16, 2023
Revised: Mar. 02, 2024
Accepted: Mar. 22, 2024

Supplementary Material

Supplementary material accompanies this paper.

Figure S1: Distribution of chemical elements map a) SEP-2:simples sample both with sepiolite b) 0.5/0.10/2: grafting sample both with sepiolite.

Figure S2: Photographs from SEM of LDPE-2 composition.

Figure S3: Photographs from SEM of gLDPE-2 composition

Figure S4: Photographs from SEM of SEP-2 composition.

Figure S5: Photographs from SEM of 0.5/0.10/2 composition.

Figure S6: Tensile versus strain curve – median sample.

Figure S7:TGA/DTG curves of 0.5/0.05/0 composition.

Figure S8:TGA/DTG curves of 0.5/0.05/2 composition.

Figure S9:TGA/DTG curves of 0.5/0.10/2 composition.

Figure S10: TGA/DTG curves of 0.5/0.10/2 composition.

Figure S11: TGA/DTG curves of 0.75/0.075/1 composition.

Figure S12: TGA/DTG curves of 1.0/0.05/2 composition.

Figure S13: TGA/DTG curves 1.0/0.05/0 composition.

Figure S14: TGA/DTG curves 1.0/0.10/0 composition.

Figure S15: TGA/DTG curves 1.0/0.10/2 composition.

This material is available as part of the online article from https://doi.org/10.1590/0104-1428.20230059